Solvent-Based Fatty Alcohol Synthesis Using Supercritical Butane. Thermodynamic Analysis

D.S. Brands, E.K. Poels, A.C. Dimian, and A. Bliek*
Department of Chemical Engineering, University of Amsterdam, 1018WV Amsterdam, The Netherlands

ABSTRACT: Conventional liquid-phase fatty ester hydrogenolysis processes are necessarily operated at high pressures owing to the limited solubility of hydrogen in the reaction medium. In a solvent-based process this problem can be overcome, but recycling and product–solvent separation may turn out to be difficult. An alternative is the use of supercritical solvents, for which the solubility of fatty esters and fatty alcohols is high. Dropping the pressure into the subcritical domain allows for easy product separation and reactant recycle. In the present work we have analyzed the hydrogenolysis of methyl palmitate in supercritical butane. A reliable estimation of properties of the supercritical mixture can be obtained by fitting experimental vapor–liquid equilibrium data with Schwatzentruber–Renon cubic equation of state. The reaction mixture remains supercritical for a maximum pressure of 9 MPa and temperature of 470 K for mole fractions of hydrogen and methyl palmitate of 0.1 and 0.025, respectively. In these conditions an equilibrium conversion of more than 99% can be reached. An industrial process is feasible.

Paper no. J9819 in *JAOCS 79,* 75–83 (January 2002).

KEY WORDS: Butane, fatty alcohols, hexadecanol, hydrogenolysis, methyl palmitate, solvent, supercritical.

The industrial route from natural fats and oils to fatty alcohols generally proceeds *via* hydrolysis of triglycerides to fatty acids, esterification to methyl esters, and hydrogenolysis of methyl esters to fatty alcohols (1). The last step is usually a catalytic process carried out in slurry or fixed-bed reactor using hydrogen between 20 and 30 MPa (2,3). Such high pressure is required in view of the low solubility of hydrogen in the methyl ester, and because of limitations of chemical equilibrium and catalyst activity.

High operating pressures and a very large excess of hydrogen, 20 to 100 times the amount of fatty acid, seriously affect capital and operating costs. This explains the efforts made to arrive at low-pressure processes and low hydrogen-to-ester molar feed ratios.

Oleofina (4) developed a special catalyst for a liquid-phase process at pressures below 6 MPa. Few details about the catalyst have been disclosed, and to our knowledge this process and catalyst have not been commercialized.

Davy McKee Corporation reported promising developments (5). Using a vapor-phase process, they claim to obtain full methyl ester conversion at 0.7–7 MPa. The main disadvantage of this process lies in the fact that it relies on the volatility of the fatty ester feed. Especially C_{16} and C_{18} esters have such low vapor pressures that an excessive hot hydrogen recycle is required for their vaporization.

In our group, a liquid-phase ester hydrogenolysis process based on an inert solvent was investigated (6). Small linear alkanes such as octane or high-boiling mineral white oil are suitable solvents. These solvents act as hydrogen carriers and allow fairly high hydrogen-to-ester molar ratios. By using solvents such as octane in combination with highly active $Cu/ZnO/SiO_2$ catalysts, full conversion could be reached at hydrogen pressures as low as 8 MPa. Because of the low hydrogen pressure, by-product formation is small; only 0.5% of hydrocarbons are formed. Wax ester formation is slightly higher (4.5%), but they can be recycled and hydrogenated to the desired alcohol, the overall selectivity being better than 99%. Whereas the conversion achievable in a solvent-based process is very high, the basic problem is large solvent recycle and additional solvent–product separation. This is to be regarded as a serious disadvantage.

Ester hydrogenolysis using a supercritical solvent. Supercritical fluids are predominantly used in the extraction of low-volatility natural compounds, as fragrances and flavors, decaffeination of coffee beans, extraction of oil from oilseeds, etc. The advantage of supercritical extraction over conventional extraction arises from the strong variation of the solubility of some large molecules in supercritical solvents around the critical point. The high solubility of natural materials such as fatty esters in supercritical solvents and the energy-efficient product–solvent separation may render a supercritical solvent-based ester hydrogenolysis process economically viable.

Scope of work. To assess the feasibility of an industrial process for solvent-based ester hydrogenolysis in supercritical conditions, we need to consider the reactor, separations, and recycles in an integrated manner. It is of paramount importance to have a reliable description of the thermodynamic properties under both supercritical and subcritical conditions. Some of the required binary interaction parameters data were not available, and thus they were fitted from experimental vapor–liquid equilibrium data. Also, the availability and accuracy of pure component properties and property estimation methods are discussed. The selection of a suitable solvent is based on: (i) being chemically inert toward fatty methyl esters and products, (ii) having high solubility of fatty esters and hydrogen, (iii) having a low critical temperature and pressure (T_c and P_c), and (iv) having a low price and easy handling. Small alkanes

---

*To whom correspondence should be addressed at Department of Chemical Engineering, Nieuwe Achtergracht 166, 1018WV Amsterdam, The Netherlands. E-mail: bliek@its.chem.uva.nl

TABLE 1
Physical Properties of Some Small Hydrocarbons.

Hydrocarbon	NBP (K)	T_c (K)	P_c (10^5 Pa)
Methane	111.6	190.4	46.0
Ethane	184.6	305.4	48.8
Propane	231.1	369.8	42.5
Butane	272.7	425.1	38.0
Pentane	309.2	469.7	33.7
Hexane	341.9	507.5	30.1

[a] Normal boiling point.

have the right supercritical properties (Table 1) and thus are potential candidates. As the P_c decreases and the T_c increases with the number of carbon atoms, large alkanes obviously cannot be used. Too-high temperatures result in low reaction selectivity due to overhydrogenation to hydrocarbons. The optimal temperature for fatty ester hydrogenolysis lies around 470 K. Hydrocarbons beyond C_5 have a critical temperature above this value and are not suitable. The smallest alkanes show a somewhat higher P_c, which could diminish the advantages of a solvent-based process.

A good compromise with respect to T_c and P_c is found in butane, which is available at low cost and is easy to store, transport, and handle.

METHODS

(i) Experimental procedures: Bubble point measurements. Bubble point measurements were performed in the so-called Cailletet apparatus described elsewhere (7). The temperature was measured with an accuracy of ±0.01 K, and the bubble pressure was better than 0.005 MPa.

Chemicals. Methyl palmitate and hexadecanol p.a. were purified by washing with sodium hydroxide and drying with sodium sulfate, followed by vacuum distillation to a purity of greater than 99.95%, as determined by titration and gas chromatographic (GC) analysis.

Simulation package. All data regression, property calculations, and simulations were performed by using Aspen Plus™ process simulator version 9.3 (8).

(ii) Thermodynamic models for description of physical properties. Cubic equation of state (EOS) methods allow for the prediction of thermodynamic properties in the supercritical region, even when only subcritical experimental data are available. The two equations of state used for prediction of vapor–liquid equilibria are shown in Table 2, i.e., those by Peng and Robinson (9) and Schwartzentruber and Renon (SR) (10). The unary and binary parameters involved

TABLE 2
Peng–Robinson and Schwartzentruber–Renon Equations of State

Peng–Robinson	Schwartzentruber–Renon
Equations of state	
$P=\dfrac{RT}{V_m-b}-\dfrac{a}{V_m\left(V_m+b\right)+b\left(V_m-b\right)}$ [1]	$P=\dfrac{RT}{V_m+c-b}-\dfrac{a}{\left(V_m+c\right)\left(V_m+c+b\right)}$ [7]
Mixing rules	
$a=\sum_i\sum_j x_ix_j\left(a_ia_j\right)^{0.5}\left(1-k_{ij}\right)$ [2]	$a=\sum_i\sum_j x_ix_j\left(a_i+a_j\right)^{0.5}\left[1-k_{ij}-l_{ij}\left(x_i-x_j\right)\right]$ [8]
$b=\sum_i x_ib_i$ [3]	$b=\sum_i\sum_j x_ix_j\dfrac{b_i+b_j}{2}$ [9]
	$c=\sum_i x_ic_i$ [10]
	$k_{ij}=k_{ij}^0+k_{ij}^1T+k_{ij}^2/T$ [11]
	$l_{ij}=l_{ij}^0+l_{ij}^1T+l_{ij}^2/T$ [12]
Pure component parameters[a]	
$a_i=\dfrac{0.45724\cdot R^2T_{c,i}^2}{P_{c,i}}\left[1+f_i\left(\omega_i\right)\left(1-T_{r,i}^{0.5}\right)\right]^{2\,*}$ [4]	
$b_i=\dfrac{0.07780\cdot RT_{c,i}}{P_{c,i}}^{*}$ [5]	
$f_i\left(\omega_i\right)=0.37464+1.545226\cdot\omega_i-0.26992\cdot\omega_i^{2\,*}$ [6]	

[a] The relations used to calculate the pure component parameters a_i, b_i, and c_i for the Schwartzentruber–Renon equation are similar, but contain additional parameters that can be fitted from experimental data. *Please note that the numerical constants in Equations 7–9 are valid for S.I. units only.

in models have been identified by regression of experimental equilibrium data.

A considerable amount of literature is available on the behavior of fats, oils, and their derivatives in supercritical solvents, mostly carbon dioxide (11–14). Zou *et al.* (15) reports phase-equilibrium data for sub- and supercritical mixtures of methyl oleate (C_{18} methyl ester) and ethane. Experimental data were convincingly shown to match the predictions of the Peng–Robinson EOS, but the binary interaction parameters were found to be temperature dependent.

The SR EOS has been suggested as accurate for high pressures and nonideal mixtures. The improvement consists of increased accuracy of pure-component vapor pressure by additional parameters, as well as of more powerful mixing rules. Two types of interaction parameters, k_{ij} and l_{ij}, are used to describe more accurately the concentration effects (see Table 2). Both are temperature dependent, as a polynomial of T and $1/T$, so that up to six binary interaction parameters can be considered. In practice, four should suffice, these being k_{ij}^0 and l_{ij}^0 plus either k_{ij}^1 and l_{ij}^1 or k_{ij}^2 and l_{ij}^2.

The equilibrium conversion has been calculated by minimizing the Gibbs free energy of reaction. By using an EOS, it is possible to calculate the departure function $G\text{-}G°$. Similarly, for the calculation of reaction enthalpy, the departure function can be defined as $H\text{-}H°$. Enthalpy and entropy of formation are conventionally reported for components in the ideal-gas state at 298 K. At other temperatures, a heat-capacity function is added to the enthalpy and entropy at 298 K. In this work the departure functions have been calculated using the Lee–Kesler EOS.

RESULTS

Pure component data. Table 3 presents pure component data. For butane, methanol, hexadecanol, and hexadecane, reliable values of the P_c, T_c, and acentric factor are available, but not for methyl palmitate. Several group contribution methods can be used to estimate these parameters, but most of these require accurate values of the normal boiling point. In Reference 16, a boiling point of 418°C at 99.35 kPa is reported for methyl palmitate. This value is far above the decomposition temperature and may have been obtained by extrapolation from reduced-pressure measurements. Krop *et al.* (17) reported a boiling point of 322°C (at 744 mm Hg) for methyl palmitate using a GC method and Kováts retention indices.

To assess the estimation methods for the T_c of long-chain esters, the available experimental data on the T_c for methyl laurate (a C_{12} methyl ester) were tested against the calculated values using the empirical Ambrose, Joback, Lydersen, and Fedors methods (18), respectively (see Table 4). Clearly, for methyl laurate the Ambrose and Lydersen methods yield the best estimate of T_c and P_c, respectively, with a deviation around 1%. As a consequence, these methods were applied to estimate T_c and P_c for methyl palmitate (Table 3). The acentric factor was estimated using the Lee–Kesler method (19).

For cetyl palmitate, also referred to as wax ester, it is particularly difficult to obtain reliable pure component data. Its normal boiling point and T_c lie far above the temperature of decomposition. Weast *et al.* (20) report a value of T_b = 360°C which seems unrealistically low when compared to methyl palmitate (T_b = 322°C).

TABLE 3
Pure Component Data[a]

Compound	Abbr.	M_W (g/mol)	NBp (K)	T_c (K)	P_c (10^5Pa)	Z_c	ω	mp (K)
Methyl palmitate ($C_{17}H_{34}O_2$)	MePa	270.46	595.15[b]	752.65[c]	13.89[c]	0.225[d]	0.895[e]	303[f]
Hydrogen	H_2	2.02	20.39	33.19	13.13	0.305	–0.2159	14.0[g]
Methane	CH_4	16.04	111.66	190.56	45.99	0.286	0.01155	90.7[g]
Hexadecanol ($C_{16}H_{34}O$)	C_{16}alc	242.45	597.23	770.00	16.10	0.228	0.81628	323.15[f]
Methanol	MeOH	32.04	337.85	512.64	80.97	0.224	0.5639	175.5[g]
Cetyl palmitate ($C_{32}H_{64}O_2$)	Wax	480.86	807.15[h]	965.45[h]	7.87[c]	0.1817[d]	1.0237[e]	326–327[f]
Hexadecane ($C_{16}H_{34}$)	Hedeca	226.45	560.01	723.00	14.00	0.22	0.7174	291.35[f]
Water	H_2O	18.02	373.15	647.13	220.055	0.229	0.3448	273.15[g]
Butane (C_4H_{10})	Butane	58.12	272.65	425.12	37.96	0.274	0.2001	134.8[g]
Ethylene glycol ($C_2H_6O_3$)	Glycol	62.07	470.45	719.70	77.00	0.246	0.48683	260.15
Hexane	Hexane	86.18	341.88	507.6	30.25	0.266	0.3012	177.8[g]
Isobutane	Iso	58.12	261.43	408.14	36.48	0.282	0.1807	113.6[g]

[a] All values were retrieved from the Aspen Plus database except where indicated. M_W, molecular weight; NBP, normal boiling point; T_c, critical temperature; P_c, critical pressure; Z_c, critical compressibility; ω, acentric factor.
[b] Taken from Reference 17.
[c] Estimated using the Ambrose method (18).
[d] Calculated using the definition method (18).
[e] Estimated using the Lee–Kesler method (18).
[f] Taken from Reference 18.
[g] Taken from Reference 18.
[h] Estimated using the American Petroleum Institute method (21).

TABLE 4
Evaluation of Estimation Methods for Critical Temperature and Pressure of Methyl Laurate

Parameter	Value	Difference (%)	Estimation method
Critical temperature	712 K	—	Measured
	701.64 K	–1.46	Joback
	707.29 K	–0.66	Ambrose
	699.82 K	–1.71	Lydersen
	721.34 K	+1.31	Fedors
Critical pressure	17.40 Bar	—	Measured
	16.51 Bar	–5.11	Joback
	17.29 Bar	–0.63	Ambrose
	17.39 Bar	–0.06	Lydersen

Group contribution methods yield less and less reliable results for hydrocarbons with increasing chain length since they are optimized for small (alkane) molecules. This is illustrated in Table 5, showing data and estimations of P_c and T_c of dotriacontane, a linear C_{32} alkane. The values of T_b and T_c are more or less overestimated, while the accuracy in the estimation of P_c strongly depends on the method used. Furthermore, the estimated value of the T_c lies below that of the boiling temperature as determined using Joback's method. An alternative approach, published by the American Petroleum Institute (API) (21), relates properties like T_b, T_c, and P_c to that of alkane analogs based on known parameters like molecular weight and density. Since with increasing chain length wax esters behave like alkanes, this approach looks promising. Based on density (0.8324 g/cm^3) and molecular weight, values of T_b = 807 K and T_c = 965 K were found for cetyl palmitate.

A proprietary method (Vreeswijk, J., personal communication, Unichima, The Netherlands, 1997) that uses group contributions fitted from a data set of 29 different fatty acids, esters, and alcohols in the C_8–C_{18} range was also evaluated. The maximal absolute error in boiling point for this method is 8 K, and the standard deviation 3.5 K for the 29 substances tested. This method yields a normal boiling point of 804 K for cetyl palmitate, surprisingly close to the value obtained using the API method discussed above (807 K). For methyl palmitate, a value of 588 K was found, again quite close to the value of 595 K reported by Krop *et al.* (17). Since no discrepancies between the API and the proprietary method were found, and the API method is available in open literature, it was decided to opt for this method in estimating the critical and boiling temperature of cetyl palmitate. The P_c of cetyl palmitate was estimated using the Ambrose method because of the fair estimation of the P_c of dotriacontane, see Table 5.

TABLE 5
Evaluation of Physical Property Estimation Methods for Dotriacontane ($C_{32}H_{66}$)

Parameter	Value	Difference (%)	Estimation method
Boiling temperature	738.85 K	—	Measured
	931.56 K	26.08	Joback
Critical temperature	855 K	—	Measured
	918.85 K	7.47	Joback
	869.44 K	1.69	Ambrose
	926.57 K	8.37	Lydersen
	878.08 K	2.70	Fedors
Critical pressure	7.50 bar	—	Measured
	5.43 bar	–27.60	Joback
	7.87 bar	4.93	Ambrose
	7.90 bar	5.33	Lydersen

(i) Estimation of ΔG_f^0 *and* ΔH_f^0. For the computation of Gibbs free energies and reaction enthalpies, accurate values of the standard enthalpy of formation ΔH_f^0 and standard Gibbs free energy of formation ΔG_f^0 must be available. These can be found for all components except for methyl palmitate and cetyl palmitate, which have been estimated by using the group contribution methods of Joback or Benson (18).

For increased accuracy, literature data of a chemically equivalent reference molecule as methyl laurate are used as starting point. Extrapolations are conducted according to Joback or Benson group contribution values. Table 6 presents the results.

Binary interaction parameters. In the present study the following key binaries were selected: butane + methyl palmitate, butane + hexadecanol, butane + hydrogen, butane + methanol, and hydrogen + methanol. The butane + hydrogen and butane + methyl palmitate interactions are particularly important because they are needed to estimate P_c and T_c of the mixture that enters the reactor. Other interactions are neglected, because they should not influence the process.

(i) Methyl palmitate + butane and hexadecanol + butane. For these mixtures, literature data are absent. In view of their importance, it was decided to measure bubble points of these mixtures. The results of measurements are shown in Figures 1 and 2 (numerical values can be found in Tables 7 and 8). Three critical points were measured, as indicated in Figures 1 and 2. The focus is on the region of low methyl palmitate solubility in butane, where measurements for X_{MePa} = 0.0234, 0.0540, and 0.0708 were done. For the binary system hexadecanol + butane, again measurements were performed at low concentrations.

First, experimental data were fitted using the Peng–Robinson EOS with conventional mixing rules (see Table 2). Results are shown in Table 9. It was difficult to fit the complete data set. Especially in the region near the critical point, the Peng–Robinson EOS overestimates the pressure. To evaluate the influence of temperature on the binary interaction parameter, smaller subsets of data were also regressed. As is apparent from Table 9 that the binary interaction parameter is small and its value decreases with temperature, i.e., a temperature

TABLE 6
Estimates of ΔH_f^0 and ΔG_f^0 of Methyl Palmitate and Cetyl Palmitate

Compound	ΔH_f^0 (kJ·mol^{-1})	ΔG_f^0 (kJ·mol^{-1})
Methyl palmitate	–695.0[a]	–206.0[b]
Cetyl palmitate	–1020.0[a]	–80.0[b]

[a] Using Benson's group contribution method.
[b] Using Joback's group contribution method (16); both methods use methyl laurate as a reference.

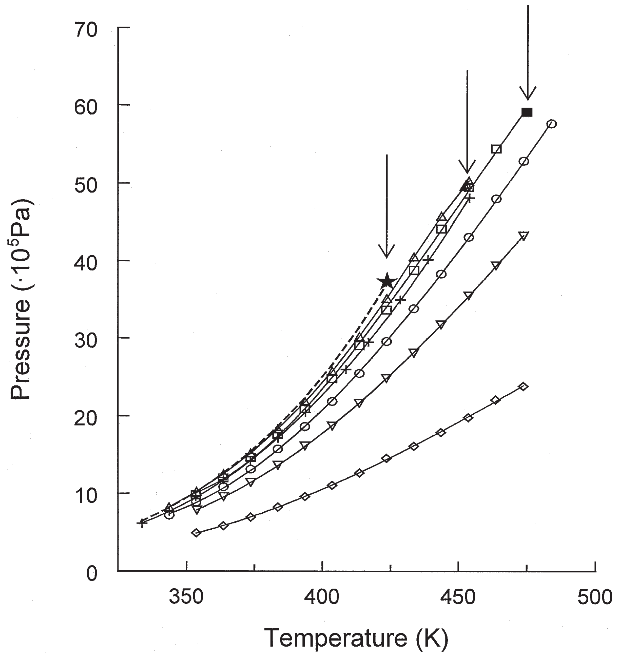

FIG. 1. Bubble points of methyl palmitate + butane mixtures. Variable: methyl palmitate mole fraction. - - - -: 0.000; △: 0.0234; □: 0.0540; +: 0.0708; ○: 0.1373; ▽: 0.249; ◇: 0.5053. Closed symbols, arrows: critical points.

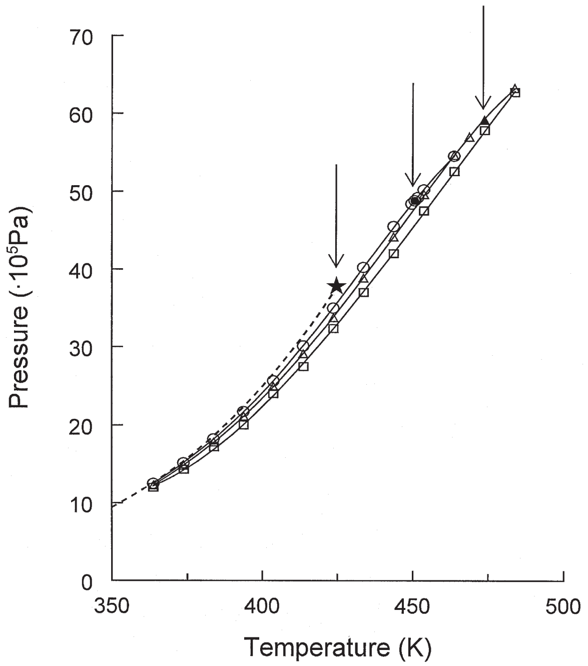

FIG. 2. Bubble points of the hexadecanol + butane mixture. Variable: hexadecanol mole fraction. - - -: 0.000; ○: 0.0249; △: 0.0498; □: 0.0995. Closed symbols, arrows: critical points.

dependency for the binary interaction parameter exists. For methyl oleate + butane mixtures, similar values of the binary parameter have been reported, showing a similar temperature dependence (15).

As it is essential to correctly assess the critical point over the entire temperature range studied, the same data set was regressed using the SR EOS, since its binary interaction parameters can be temperature dependent. The influence of the volume translation parameter *c* is expected to be small. Hence, it was omitted from the regression.

For the methyl palmitate + butane mixture, a good fit of the data set was obtained when only three parameters k_{ij}^0, k_{ij}^2, and l_{ij}^0 were identified, with all other parameters set to zero. A slightly better fit is obtained with inclusion of a fourth binary parameter (l_{ij}^2), but the differences were so small that it was decided to disregard this parameter. The results, shown in Table 10, reveal a fair fit to experimental data and low values of the RMS in temperature and pressure.

Table 10 also shows the results for the hexadecanol + butane mixture. A fair fit of the data set is obtained when only

TABLE 7
Bubble Point Data of the Methyl Palmitate + Butane Mixture

$X_{\mathrm{MePa}} = 0.0234$		$X_{\mathrm{MePa}} = 0.054$		$X_{\mathrm{MePa}} = 0.0708$		$X_{\mathrm{MePa}} = 0.1373$		$X_{\mathrm{MePa}} = 0.2485$		$X_{\mathrm{MePa}} = 0.5053$	
T (K)	*P* (·10^5 Pa)	*T* (K)	*P* (·10^5 Pa)	*T* (K)	*P* (·10^5 Pa)	*T* (K)	*P* (·10^5 Pa)	*T* (K)	*P* (·10^5 Pa)	*T* (K)	*P* (·10^5 Pa)
343.69	8.242	353.66	9.81	333.78	6.16	343.73	7.20	353.78	7.86	353.63	4.91
353.68	10.24	363.62	12.01	343.75	7.71	353.64	8.90	363.70	9.56	363.60	5.86
363.64	12.54	373.61	14.66	353.41	9.56	363.65	10.85	373.65	11.41	373.59	6.96
373.66	15.24	383.59	17.66	363.60	11.76	373.64	13.15	383.63	13.66	383.58	8.26
383.64	18.34	393.61	21.01	373.56	14.26	383.62	15.75	393.63	16.16	393.58	9.61
393.65	21.84	403.57	24.81	383.61	17.16	393.61	18.65	403.64	18.71	403.57	11.06
403.64	25.79	413.59	29.06	393.82	20.46	403.62	21.90	413.62	21.66	413.58	12.66
413.66	30.24	423.58	33.66	408.69	26.01	413.63	25.50	423.60	24.86	423.59	14.56
423.67	35.19	433.61	38.81	416.95	29.51	423.61	29.60	433.60	28.11	433.59	16.11
433.70	40.54	443.67	44.16	428.69	35.01	433.63	33.85	443.64	31.76	443.62	17.91
443.67	45.79	453.65	49.51	438.82	40.16	443.65	38.35	453.65	35.56	453.60	19.81
451.81	49.49[a]	463.65	54.46	453.93	48.16	453.68	43.10	463.69	39.41	463.57	22.11
452.20	49.64[b]	474.72	59.16[a]			463.70	48.05	473.65	43.26	473.59	23.86
452.71	49.89[b]					473.68	52.90				
453.70	50.34[b]					483.74	57.70				

[a] Critical point.
[b] Dew point.

TABLE 8
Bubble Point Data of the Hexadecyl Alcohol + Butane Mixture

$X_{\text{hexalc}} = 0.0249$		$X_{\text{hexalc}} = 0.0498$		$X_{\text{hexalc}} = 0.0995$	
T (K)	*P* ($\cdot 10^5$ Pa)	*T* (K)	*P* ($\cdot 10^5$ Pa)	*T* (K)	*P* ($\cdot 10^5$ Pa)
363.71	12.52	363.75	12.32	363.70	11.99
373.66	15.17	373.71	14.82	373.80	14.34
383.63	18.22	383.68	17.82	383.80	17.19
393.61	21.72	393.68	21.12	393.73	19.99
403.59	25.67	403.64	24.97	403.65	24.04
413.61	30.12	413.63	29.12	413.70	27.49
423.59	35.02	423.65	33.82	423.70	32.39
433.59	40.27	433.63	38.87	433.69	37.04
443.60	45.57	443.64	44.22	443.70	42.09
449.58	48.47	453.67	49.67	453.72	47.59
450.63	48.87[a]	463.66	54.72	463.75	52.64
451.63	49.27[b]	468.65	57.07	473.75	57.89
453.62	50.27[b]	473.66	59.22[a]	483.73	62.79
463.64	54.62[b]	483.65	63.32[b]		
473.65	58.32[b]				

[a] Critical point.
[b] Dew point.

the parameters k_{ij}^0 and k_{ij}^2 are identified; see Table 10. All other parameters are set to zero, implying that for higher temperatures the binary interaction parameter k_{ij}^1 drops. Because of the better fit of the experimental bubble pressure data, it was decided to use the SR EOS for fitting all the experimental vapor liquid equilibrium (VLE) data.

(ii) Butane + hydrogen. For this system, a good source of equilibrium VLE data is available (22). A satisfactory fit of the data using the SR EOS could be obtained using only k_{ij}^0 and l_{ij}^0. The use of temperature-dependent binary parameters did not improve the fit. The fact that incorporating l_{ij}^0 yields a better fit indicates a concentration dependency of the binary interaction parameters. Regression results are shown in Table 10.

(iii) Butane + methanol. Literature data are available for the butane + methanol system (23). A good coverage of the data was obtained with incorporation of the parameters k_{ij}^0, k_{ij}^2, and l_{ij}^0. This implies a positive order of the binary interaction parameter k_{ij} in temperature. The fit obtained was good, as shown by the standard deviations (Table 10).

(iv) Methanol + hydrogen. Several sources of data are available for the methanol + hydrogen mixture (24–26). The most consistent data sets (25,26) were fitted with the SR EOS. However, it was not possible to obtain reliable binary interaction parameters. Therefore, it was decided to ignore the binary interaction parameter for the methanol + hydrogen system. For the physical properties of the reaction mixture itself, no significant effects are expected.

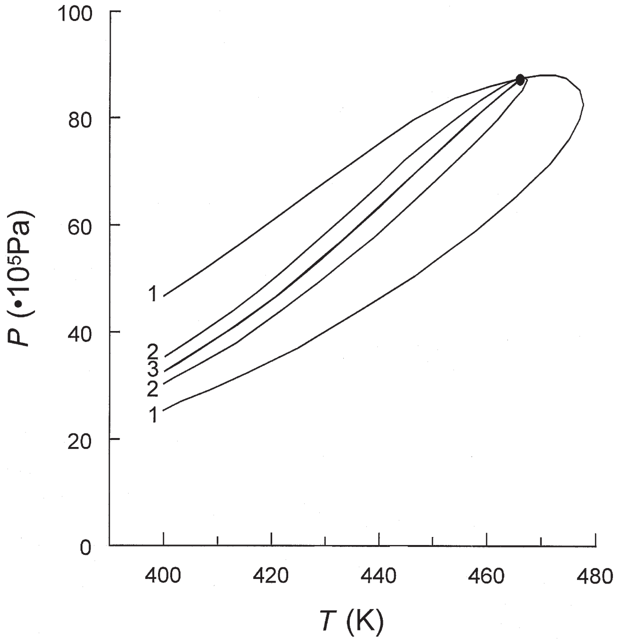

FIG. 3. Determination of T_c and P_c for the reaction mixture using pressure envelopes at different vapor fractions. The composition of the mixture is indicated in Table 12. Variable: Vapor fraction. Curve 1: 0.8; curve 2: 0.6; curve 3: 0.5; ●: critical point.

Lee–Kesler binary interaction parameters. This EOS is used to calculate the departure functions of the Gibbs free energy and the enthalpy. Binary interaction parameters of key components for this EOS were determined with the same data sets and in a similar way as was done for the SR EOS. Results are shown in Table 11.

Critical properties of the reaction mixture. To estimate P_c and T_c for different reaction mixtures, Pressure–temperature envelopes have been calculated (see Fig. 3). Because of the better fit, it was decided to use the SR EOS to estimate critical properties of our system.

As is apparent from Figures 4 and 5, both T_c and P_c

TABLE 9
Regression of the Peng–Robinson EOS Binary Interaction Parameter for the Methyl Palmitate + Butane and Hexadecanol + Butane Mixture[a]

Mixture	Temperature range	# Data points	k_{ij}	Standard deviation	RMS in *T* (%)	RMS in *P* (%)
Methyl palmitate + butane	All data points	35	0.0203	$4.5 \cdot 10^{-4}$	$7.4 \cdot 10^{-4}$	0.35
	333–393 K	18	0.0426	$9.4 \cdot 10^{-3}$	$1.7 \cdot 10^{-3}$	1.26
	403–433 K	12	$-3.622 \cdot 10^{-3}$	$1.3 \cdot 10^{-3}$	$1.2 \cdot 10^{-3}$	0.34
	Above 433 K	5	–0.0127	$6.4 \cdot 10^{-3}$	$9.1 \cdot 10^{-5}$	0.03
Hexadecanol + butane	All data points	35	–0.0753	$1.23 \cdot 10^{-2}$	$9.8 \cdot 10^{-3}$	3.51
	333–393 K	12	0.0572	$9.7 \cdot 10^{-3}$	$2.3 \cdot 10^{-3}$	1.34
	403–433 K	12	0.0209	$5.4 \cdot 10^{-4}$	$5.5 \cdot 10^{-5}$	0.18
	Above 433 K	11	$1.04 \cdot 10^{-3}$	$1.2 \cdot 10^{-2}$	$1.7 \cdot 10^{-4}$	0.03

[a] EOS, equation of state; RMS, root mean of squares.

TABLE 10
Binary Parameters for the Schwartzentruber–Renon EOS for the Methyl Palmitate + Butane, Hexadecanol + Butane, Butane + Hydrogen, and Butane + Methanol Mixture[a]

Mixture	# Data points	RMS in T (%)	RMS in P (%)	Parameter	Value	Standard deviation
Methyl palmitate + butane	34	$1.0 \cdot 10^{-4}$	$3.7 \cdot 10^{-2}$	k_{ij}^0	–0.2972	$5.38 \cdot 10^{-3}$
				k_{ij}^2 (°C)	120.8	1.97
				l_{ij}^0	$1.274 \cdot 10^{-2}$	$1.56 \cdot 10^{-3}$
Hexadecanol + butane	35	$2.1 \cdot 10^{-4}$	$12 \cdot 10^{-2}$	k_{ij}^0	–0.1893	0.020
				k_{ij}^2 (°C)	79.17	8.01
Butane + hydrogen	60	$1.3 \cdot 10^{-4}$	$2.3 \cdot 10^{-4}$	k_{ij}^0	–0.1883	$3.53 \cdot 10^{-2}$
				l_{ij}^0	0.4697	$5.7 \cdot 10^{-2}$
Butane + methanol	23	$5.0 \cdot 10^{-2}$	$1.0 \cdot 10^{-2}$	k_{ij}^0	0.5195	$4.26 \cdot 10^{-2}$
				k_{ij}^2 (°C)	–137.44	15.01
				l_{ij}^0	0.131	$1.04 \cdot 10^{-2}$

[a] See Table 9 for abbreviations.

TABLE 11
EOS Parameters for the Lee–Kesler EOS[a]

Mixture	k_{ij}	Standard deviation
Methanol + butane	–0.0902	$7.07 \cdot 10^{-3}$
Methyl palmitate + butane	0.1217	$1.57 \cdot 10^{-2}$
Hexadecanol + butane	0.2056	$5.09 \cdot 10^{-3}$
Hydrogen + butane	1.4705	$4.31 \cdot 10^{-2}$

[a] See Table 9 for abbreviation.

increase for higher concentrations of methyl palmitate and hydrogen. Excessive operating temperatures give overhydrogenation of the product alcohols to alkanes and reduce the reaction selectivity, whereas high operating pressures would be detrimental for process economics. These constraints set limits to the maximal allowable reactant concentration.

A different representation of critical temperature and pressure is shown in Figures 6 and 7. For an upper temperature limit of 470 K (1) and an allowable pressure of 9.0 MPa, the maximal allowable feed concentration of hydrogen and methyl palmitate must be restricted, for instance to 10 and 2.5 mol%, respectively. In order to assess whether hydrogenolysis under supercritical conditions is feasible, it is necessary to (i) establish the window of feed compositions where both the feed and the product are supercritical and (ii) to assess the achievable equilibrium conversion.

Chemical equilibrium calculations. The theoretically attainable equilibrium conversion with the reaction mixture as shown in Table 12 is calculated by Gibbs free energy minimization. Figure 8 demonstrates the sensitivity of the methyl palmitate equilibrium conversion vs. pressure, temperature,

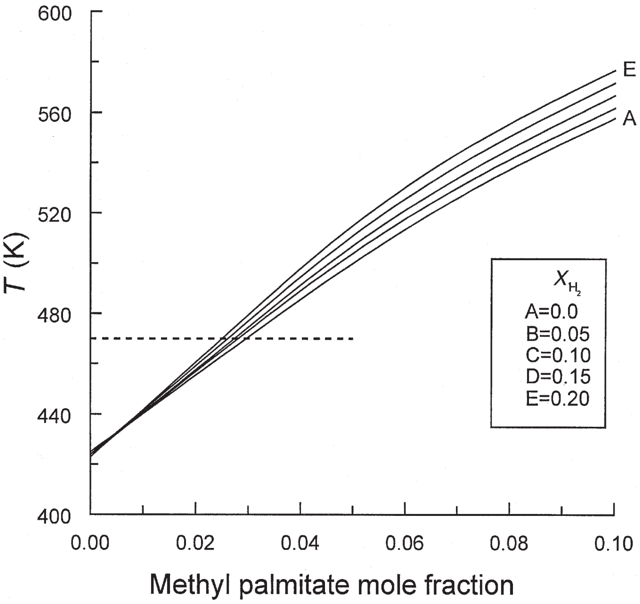

FIG. 4. Critical temperature T_c of methyl palmitate + hydrogen + butane mixtures vs. composition. Corresponding supercritical pressures are indicated in Figure 5. ------: maximum allowable reaction temperature from a reaction selectivity point of view.

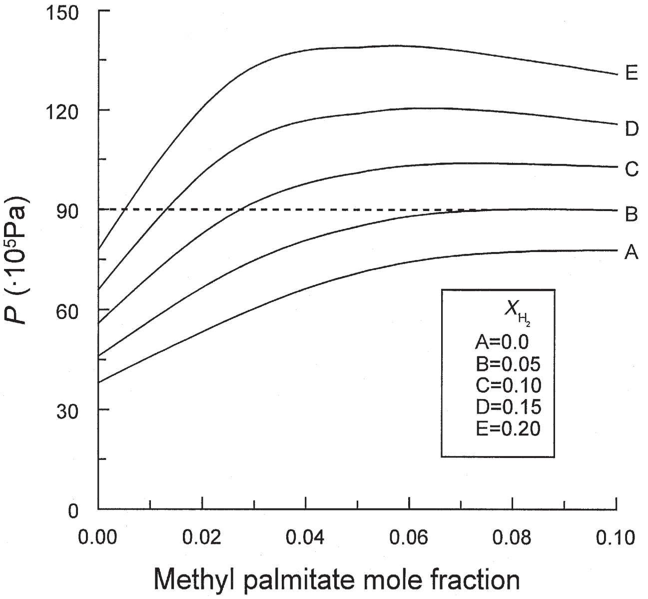

FIG. 5. Critical pressure P_c of methyl palmitate + hydrogen + butane mixtures vs. composition. Corresponding critical temperatures are indicated in Figure 4. ------ : 9 MPa pressure limit, assumed maximal allowable reaction pressure.

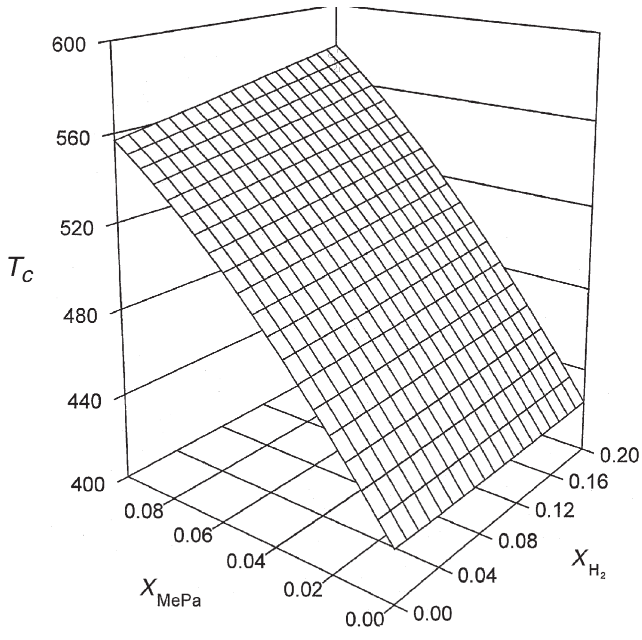

FIG. 6. Critical temperature T_c as a function of composition for a mixture of methyl palmitate, hydrogen, and butane.

and initial mole fraction of hydrogen (X_{H_2}). As a consequence of the exothermic nature of ester hydrogenolysis, the ester conversion decreases with temperature (Fig. 8A). As dictated by reaction stoichiometry, the conversion increases as a function of total pressure (Fig. 8B) and initial hydrogen mole fraction (Fig. 8C).

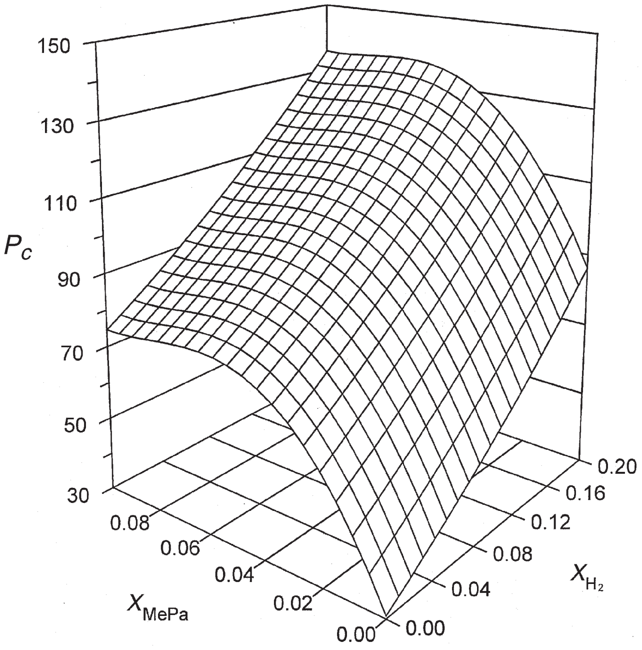

FIG. 7. Critical pressure P_c as a function of composition for a mixture of methyl palmitate, hydrogen, and butane.

TABLE 12
Input Composition of the Reaction Mixture

Component	Mole fraction	Relative amount
Methyl palmitate	0.025	1
Hydrogen	0.100	4
Butane	0.875	35

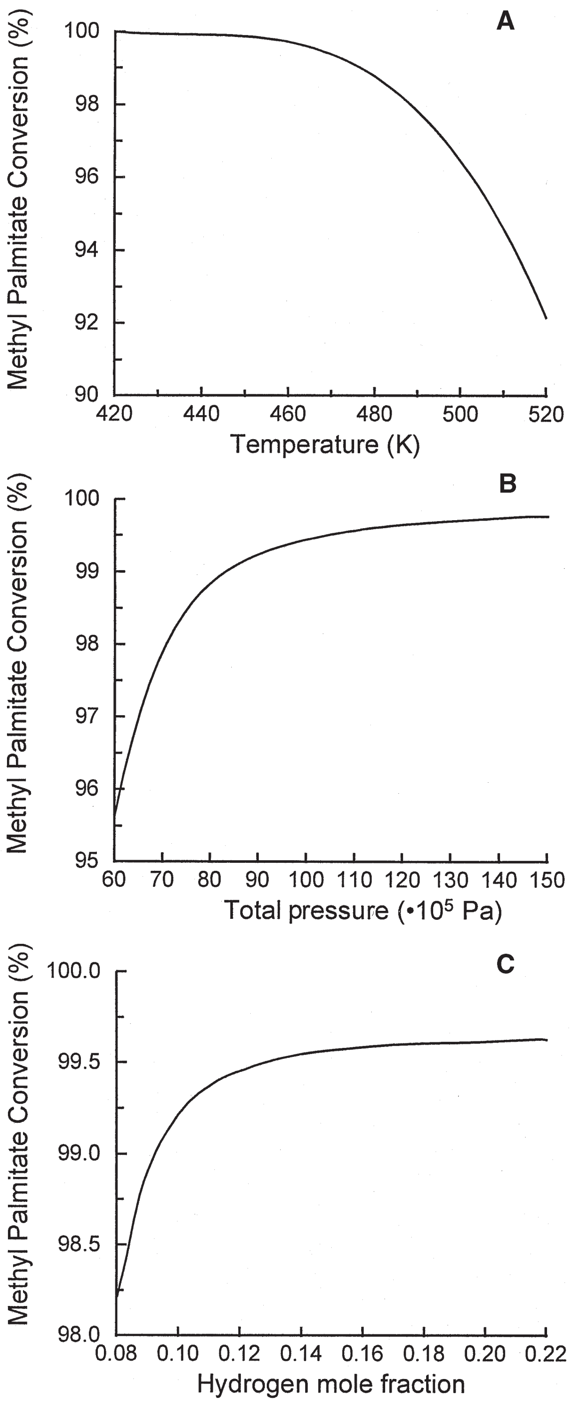

FIG. 8. Thermodynamic equilibrium conversion of methyl palmitate. Pressure is 9.0 MPa, methyl palmitate mole fraction is 0.025, hydrogen mole fraction is 0.100, and temperature is 470 K unless otherwise specified. (A) Conversion vs. temperature; (B) conversion vs. pressure; (C) conversion vs. hydrogen mole fraction in the feed.

The calculated equilibrium conversion for the mixture in Table 12 is 99.2 mol% at 470 K and 9.0 MPa. This value is certainly sufficient to attain detergent-grade fatty alcohols. One may conclude that the constraint of the feed and product flows in supercritical states does not seriously limit the achievable conversion, and from this point of view supercritical hydrogenolysis is feasible.

A reliable estimation of the thermodynamic properties of supercritical reaction mixtures can be obtained by fitting experimental bubble points by the SR EOS with concentration- and temperature-dependent mixing rules.

The behavior of mixtures of methyl palmitate + butane, as well as cetyl alcohol + butane, can be described accurately by SR EOS. Experimental data have been fitted reliably over a broad temperature and concentration range. The Peng–Robinson EOS without temperature-dependent binary interaction parameters gave less good results. For chemical equilibrium calculations, Lee–Kessler binary interaction parameters are also determined.

Supercritical data of reaction mixtures were evaluated, assuming the SR EOS and reaction equilibrium for methyl palmitate hydrogenolysis. It was verified that in supercritical butane for a maximal operating pressure of 9 MPa and a maximal reaction temperature of 470 K, the mixture remains supercritical for mole fractions of hydrogen and a methyl palmitate in the feed of typically 10 and 2.5 mol%, respectively. These values indicate the practical upper values of reactant concentrations in supercritical butane. Under these conditions, the equilibrium conversion for the hydrogenolysis reaction is 99.2%. Given this high conversion level, the hydrogenolysis of methyl palmitate in supercritical butane is basically feasible.

ACKNOWLEDGMENTS

Wim Poot and Theo de Loos are gratefully acknowledged for making it possible to carry out bubble point measurements at the Laboratory for Applied Thermodynamics and Phase Equilibria at Delft University of Technology, The Netherlands.

REFERENCES

1. Voeste, T., and H. Buchold, Production of Fatty Alcohols from Fatty Acids, *J. Am. Oil Chem. Soc. 61*:350–352 (1984).
2. Kreutzer, U.R., Manufacture of Fatty Alcohols Based on Natural Fats and Oils, *Ibid. 61*:343–348 (1984).
3. Buchold, H., Natural Fats and Oils Route to Fatty Alcohols, *Chem. Eng. 90*:42–43 (1983).
4. Hinnekens, H., Process for Reproducing Alcohols, U.S. Patent 4,728,671, Oleofina S.A. (1988).
5. Scarlet, J., and D. McKinley, New Developments in Catalysts for the Oleochemicals Industry, *Oils Fats Int. 9*:32–34 (1993).
6. Scheur, F.T.v.d., J.J. Vreeswijk, and L.H. Staal, A New Process for the Synthesis of Fatty Alcohols, in *Proceedings of the World Conference on Oilseed Technology and Utilization,* edited by T.H. Applewhite, AOCS Press, Champaign, 1993, pp. 453–457.
7. Loos, T.W.d., H.J.v.d. Kooi, and P.L. Ott, Vapor–Liquid Critical Curve of the System Ethane + 2-Methylpropane, *J. Chem. Eng. Data 31*:166–168 (1986).
8. Aspen Plus™, *User Manual,* version 9.3, Aspen Technology, Cambridge, MA, 1998.
9. Peng, D.Y., and D.B. Robinson, A New Two-Constants Equation of State, *Ind. Eng. Chem. Fund. 15*:59–64 (1976).
10. Schwartzentruber, J., and H. Renon, Development of a New Cubic Equation of State for Equilibrium Calculations, *Fluid Phase Equilib. 52*:127–134 (1989).
11. Yu, Z.-R., B. Singh, S.S.H. Rizvi, and J.A. Zollweg, Solubilities of Fatty Acids, Fatty Acid Esters, Triglycerides, and Fats and Oils in Supercritical Carbon Dioxide, *J. Supercrit. Fluids 7*:51–60 (1994).
12. Staby, A., C. Borch-Jensen, and J.M. Mollerup, Partition Coefficients and Solubility of Urea-Fractionated Fatty Acid Ethyl Esters from Fish Oil in Supercritical CO_2, *Fett Wissen. Technol. 96*:299–303 (1994).
13. Staby, A., T. Forskov, and J. Mollerup, Phase Equilibria of Fish Oil Fatty Acid Ethyl Esters and Sub- and Supercritical CO_2, *Fluid Phase Equilib. 87*:309–340 (1993).
14. Staby, A., and J. Mollerup, Solubility of Fish Oil Fatty Acid Ethyl Esters in Sub- and Supercritical Carbon Dioxide, *J. Am. Oil Chem. Soc. 70*:583–588 (1993).
15. Zou, M., S.B. Lim, S.S.H. Rizvi, and J.A. Zollweg, Vapor–Liquid Equilibria of Fatty Acid Esters in Supercritical Fluids, *Supercritical Fluid Science and Technology,* ACS Symposium Series, American Chemical Society, Washington, DC, 1989, pp. 98–110.
16. Lide, D.R., and H.P.R. Frederikse, *Handbook of Chemistry and Physics,* 78th edn., CRC Press, Boca Raton, Florida, 1997.
17. Krop, H.B., M.J.M.v. Velzen, J.R. Parson, and H.J. Govers, Determination of Environmentally Relevant Physical Chemical Properties of Some Fatty Acid Esters, *J. Am. Oil Chem. Soc. 74*:309–316 (1997).
18. Reid, R.C., J.M. Prausnitz, and B.E. Poling, *Properties of Gases and Liquids,* 4th edn., McGraw Hill, New York, 1987.
19. Lee, B.I., and M.G. Kesler, A Generalized Thermodynamic Correlation Based on Three-Parameter Corresponding States, *AIChE J. 21*:510–527 (1975).
20. Weast, R.C., M.J. Astle, and W.H. Beyer, *Handbook of Chemistry and Physics,* 67th edn., CRC Press, Boca Raton, Florida, 1986.
21. *American Petroleum Institute: Technical Data Book—Petroleum Refining,* 3rd edn., API, Washington, DC, 1977, pp. 4–13.
22. Klink, A.E., H.Y. Cheh, and E.H. Amick, The Vapour–Liquid Equilibrium of the Hydrogen-*n*-Butane System at Elevated Pressures, *AIChE J. 21*:1142–1148 (1975).
23. Petty, L.B., and J.M. Smith, Volumetric Behavior of the Methanol-*n*-Butane System, *Ind. Eng. Chem. 47*:1258–1265 (1955).
24. Suzuki, K., H. Sue, M. Itou, R.L. Smith, H. Inomata, K. Arai, and S. Saito, High-Pressure Vapor–Liquid Equilibrium Data of the 10-Component System Hydrogen, Carbon Monoxide, Carbon Dioxide, Water, Methane, Ethane, Propane, Methanol, Ethanol, and 1-Propanol at 313.4 and 333.4 K, *J. Chem. Eng. Data 35*:67–69 (1990).
25. Liu, Q., F. Takemura, and A. Yabe, Solubility of Hydrogen in Liquid Methanol and Methyl Formate at 20°C and 140°C, *Ibid. 41*:1141–1143 (1996).
26. Michels, A., W.D. Graaff, and J.V.D. Somme, Gas–Liquid Phase Equilibria in the System Methanol–Hydrogen, *Appl. Sci. Res. A4*:105–108 (1953).

[Received November 27, 2000; accepted October 25, 2001]